SURFACE AND INTERFACE ANALYSIS
Surf. Interface Anal. 2003; **35**: 151–155

SIA

Influence of carbon on the interfacial contact angle between alumina and liquid aluminum

Enrique Rocha-Rangel,[1,2] Paul F. Becher[2] and Edgar Lara-Curzio[2]*

[1] Materials Department, UAM-A, Av. San Pablo No. 180, Col Reynosa-Tamaulipas, Mexico, D.F. 02200, Mexico
[2] Metals & Ceramics Division, Oak Ridge National Laboratory, 1 Bethel Valley Rd, Oak Ridge, TN, 37831-6069, USA

Received 20 May 2002; Revised 21 November 2002; Accepted 26 November 2002

The wetting of alumina by pure liquid aluminum was investigated over the temperature range 900–1300 °C by the sessile drop method under a dynamic vacuum of 10^{-4}–10^{-5} Pa. When the substrate is carbon coated, the terminal contact angle is reduced to 40° at 1300 °C for times longer than 4500 s. In the absence of carbon, the final angle is 82° for the same conditions. Reactive wetting is suggested by the observation of undercutting of the substrate and ridge formation at the leading edge of the liquid aluminum in all carbon-coated samples. Based on energy considerations, the following is among the thermodynamically favorable reactions: $4Al + 3C \rightarrow Al_4C_3$. Possible mechanisms for the observed carbon-enhanced wettability in the system are discussed. Copyright © 2003 John Wiley & Sons, Ltd.

KEYWORDS: carbon; interfacial; contact angle; alumina; aluminum

INTRODUCTION

The interfacial phenomenon between metals and ceramics is of both scientific and engineering interest. In coating, joining and composite processing, performance is associated directly with the nature of the metal/ceramic interface. Specifically, the wetting of ceramic surfaces by liquid metals is an important phenomenon in the production of high-technology materials such as metal matrix composites (MMC) and ceramic matrix composites (CMC), where the enhancement of liquid infiltration and the control of bonding are of prime importance.[1] The aluminum–Al_2O_3 system is an ideal candidate for MMC and CMC owing to its low density and potential for achieving higher toughness and reasonable strength compared with alumina ceramics. However, the stable oxide film that protects aluminum from corrosion inhibits wetting, which makes the fabrication process quite difficult.

The wetting behavior of Al_2O_3 by liquid aluminum has been studied widely.[2–6] It has been found that the main problem affecting the wetting of Al_2O_3 by Al is the oxidation of Al.[7–9] This is due to the fact that the solubility limit of oxygen in Al is very small[10] and the equilibrium partial pressure of oxygen pO_2 in the oxidation reaction of Al is of the order of 10^{-44}Pa,[11] which is practically impossible to achieve in the majority of the experimental or industrial set-ups. Under such conditions, Al tends to oxidize continuously to form a stable condensed solid phase (Al_2O_3), which certainly influences the thermodynamics of this system. The addition of alloying elements such as Ti and Zr results in lowering of the contact angle between the metal and the ceramic.[12–15] Also, the use of a thin film of carbon has been reported to diminish the contact angle between Al and Al_2O_3 to values as low as 31°, thus improving wetting.[16]

Generally wetting experiments are interpreted in terms of the Young-Dupre equation.[17] This equation represents the balance of the horizontal forces, due to surface tension, acting upon a liquid drop in contact with a solid. Young established that the liquid in thermodynamic equilibrium in contact with a solid will assume a characteristic contact angle at the triple junction (solid–liquid–vapor), which depends on the surface energies of the liquid–vapor, solid–vapor and solid–liquid interfaces (γ_{l-v}, γ_{s-v} and γ_{s-l})

$$\cos\theta = \frac{\gamma_{s-v} - \gamma_{s-l}}{\gamma_{l-v}} \quad (1)$$

In several of the existing models, the Young equation is modified by considering the additional interfacial energy or free energy of reaction terms.[5,18–21] Other authors have developed models that predict the wetting or non-wetting behavior based on the work of adhesion or the change in the surface energy of the system[22,23]

$$W_{ad} = \gamma_{l-v}(1 + \cos\theta) \quad (2)$$

Although these models predict whether or not wetting will occur for a given system, they do not predict the rate of change in the wetting angles or the spreading of the droplet. This is complicated by the fact that a reaction layer also can form during the wetting and spreading processes. The spreading kinetics is needed to predict the minimum required for spreading so that both the spreading and the reaction product thickening can be optimized. Theoretical modeling of the spreading kinetics is a complex problem, even for non-reactive systems, because spreading

---

*Correspondence to: Edgar Lara-Curzio, Metals and Ceramics Division, Oak Ridge National Laboratory, 1 Bethel Valley Rd, Oak Ridge, TN, 37831-6069, USA. E-mail: laracurzioe@ornl.gov

is affected by many factors (e.g. surface irregularities, surface contamination, the formation of new products on the surface, alloying elements or impurities in the metal, etc.). Several spreading models consider the effects of the formation of a ridge at the triple point during reaction product formation and the succession of reaction ridges associated with droplet spreading.[24–28] In these models, the ridges mark the location of successive triple points where a ridge formed and acted as a barrier to further spreading, until the driving force became high enough to overcome the barrier. Once the driving force reaches this critical value, the drop spreads and the process repeats itself at the next triple point. Currently, the lack of reaction rate kinetics, interfacial energy and diffusion data, along with the uncertainties involved in high-temperature sessile drop experimental measurements, make it difficult to determine what mechanisms control the overall spreading process. Hence, considerably more experimental research is required on the spreading kinetics of reactive and non-reactive systems before the properties of systems containing ceramic/metal interfaces can be optimized.

The goal of the present work is to examine possible mechanisms by which carbon enhances the wettability in the Al–Al_2O_3 system.

EXPERIMENTAL

Pure Al (99.5% Alfa Aesar, USA) and 0.64 mm thick polycrystalline alumina (CoorsTek, 99.6% Al_2O_3) substrates were used as raw materials. Three different samples were prepared and the differences among them are presented in Table 1. Small cubes weighing ~0.3 g were diamond cut from Al stock bars. Substrates were diamond cut in square slices of side 1 cm. Carbon, films were deposited onto the substrate by a vapor deposition process using a sample coating device (Polaron Division, Bio-Rad E6700, USA). Each deposition cycle was ~45 s, which resulted in a carbon film thickness estimated to be ~1 μm. The sessile drop experiments were conducted using an induction heating generator (Lepel High Frequency Lab. Inc., Model T-30-3-DF-TL, USA). The experiments were conducted in a stainless-steel chamber under a controlled vacuum (10^{-4}–10^{-5} Pa) at temperatures of 900, 1000, 1100, 1200 and 1300 °C. The droplet profiles were recorded *in situ* as a function of temperature and time using a video camera (Canon L2, Japan). Liquid metal temperature was controlled with an infrared camera, (Ircon, Inc., Model MR-OR10-19C). Both the video camera and the infrared camera were sighted through quartz windows of the chamber (Fig. 1). Before the wetting experiments Al and the uncoated substrate were cleaned for 40 min in acetone by agitating in an ultrasonic bath. Contact angle measurements were made directly from images obtained from the video display using a digital camera (Olympus 350, Japan). The samples from the wetting experiments were analysed by SEM (Jeol, S-4700, Japan) and energy-dispersive spectroscopy (NORAN 457A-3SES, USA). The Al was removed from substrates to reveal the interface by etching in a distilled water–20% NaOH solution.

Table 1. Identification of the samples used in the sessile drop experiments

Sample	System	Carbon-coaled Al_2O_3
A1	Al–Al_2O_3	None
AC1	Al–Al_2O_3	1 carbon deposition cycle
AC3	Al–Al_2O_3	3 carbon deposition cycle

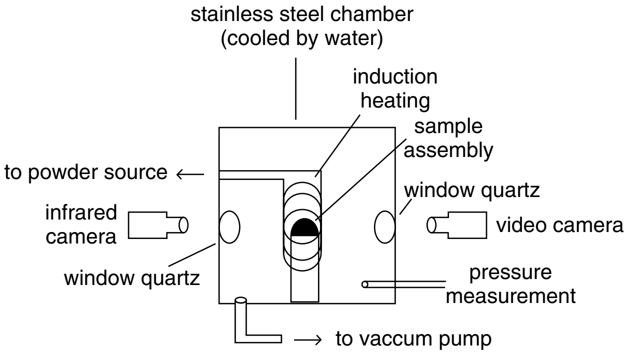

Figure 1. Schematic diagram of the experimental arrangement used for sessile drop experiments.

RESULTS AND DISCUSSION

Contact angle

Effect of temperature

The contact angle (θ) obtained after a 4500 s hold time is shown in Fig. 2 as a function of temperature for each of the samples. For each sample it was found that the contact angle decreased with increasing temperature. However, wetting of substrates by Al only occurred at temperatures at or above 1200 °C, where a required contact angle of $<90°$ (cf. Eqn (1)) was obtained. At 1300 °C, the lowest θ values were found for samples where the θ values for samples A1 and AC1 are ~83 and 80°, respectively, whereas sample AC3 exhibits a θ value of 40°. These results indicate that the deposited carbon film on the substrate plays an important role in enhancing the wetting of the alumina substrate by the molten aluminum.

Effect of time

Figure 3 shows the variation in the radius at the base of the aluminum droplet and in the contact angle as a function of time for the three samples at 1300 °C. The initial time

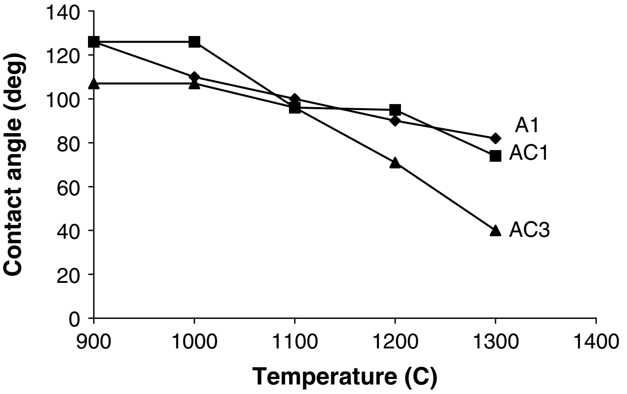

Figure 2. Final contact angle as a function of temperature.

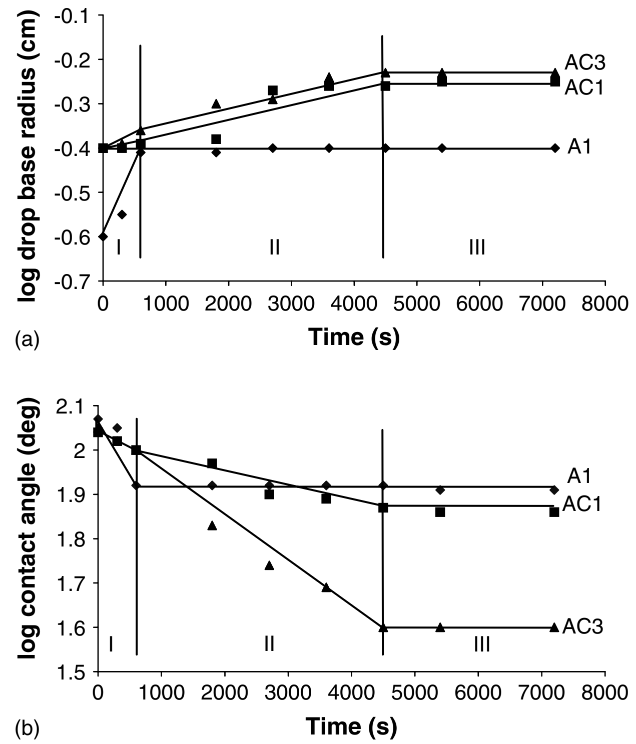

Figure 3. Variations of the drop base radius and the contact angle as a function of time.

(t_i) is chosen when liquid Al contacts the substrate and the measured test temperature reaches a constant value. For all samples the initial value of the contact angle is very high: close to 119°. For sample A1 it decreases in ~600 s to a steady value close to 83°. Laurent *et al.*[3] have studied the variation of the oxygen partial pressure with temperature for determining under which conditions the Al_2O_3 oxide layer is expected to be eroded. After several experiments that cover a wide temperature range they have assumed that, as a result of structural faults in the film and/or cracks due to the considerable thermal expansion of Al at the melting point, this Al_2O_3 film is not compact at short times and thus the following reaction can take place

$$Al_2O_3(\text{film}) + 4Al(l) \leftrightarrow 3Al_2O(g) \qquad (3)$$

Then the high value measured at $t_1 = 0$ is typical of oxidized drops and the decrease in contact angle is controlled by deoxidation of the drop,[29] which is achieved mainly by reduction of the oxide layer by liquid Al, with the production of gaseous Al_2O, as described by Eqn (3).

The contact angle obtained for sample A1 after ~600 s hold times is in good agreement with published results obtained with experimental procedures that suppress the influence of the oxide layer on wetting.[2,3] Thus, oxidation of the Al drop occurred for a short period of time in the present experimental conditions.

For samples AC1 and AC3 the contact angle plots in Fig. 3(b) consist of three stages and the wetting kinetics can be characterized by the value of the contact angle at the start of each stage.

Although the shape of the curves for both samples is very similar, faster kinetics of wetting and smaller contact angles are obtained for sample AC3 compared with sample AC1. In the first stage, the contact angle decreases from $\theta_0 = 110°$ to $\theta_1 = 79°$ for sample AC1 and from $\theta_0 = 112°$ to $\theta_1 = 55°$ for sample AC3 at t_i and $t_2 \sim 2700$ s, respectively. This first stage is similar to the kinetics obtained for sample A1. Consequently, it is likely that the mechanism that controls the kinetics of wetting during the first stage is deoxidation of the drop according to Eqn (3). At time t_2, a change in the slope of both the radius and contact angle curves is observed as the velocity of wetting decreases significantly. The second stage, between t_2 and t_3, is characterized by an almost linear change of the drop base radius and contact angle with time. Finally, during the third stage at times $t > t_3$ ($t_3 = 4500$ s), both the radius and contact angle in both samples AC1 and AC3 remain constant with time.

As can be observed in Fig. 3 for samples AC1 and AC3, the wetting kinetics is fastest during the first stage. A significant decrease in spreading rate is observed in the second stage, whereas the contact angle remains constant in the third stage. The wetting kinetics can be characterized by the values of the three contact angles (see Table 2) together with the corresponding works of adhesion (using Eqn (2)) in stages 2 and 3, respectively. The surface tension of liquid Al at 1300 °C is taken to be 0.85 J m^{-2} from the literature.[30–32]

Different researchers have reported the formation of Al_4C_3 as being responsible for the enhancement in the contact angle.[24,28] However, other researchers have reported the role of alloying elements in the metal for the same purpose.[12–15,33] Taking into consideration the time duration of the first stage and the very small concentration of impurities in the metal, the latter could not play a role in enhancing wettability. Therefore, the reactions that involve carbon are important because the contact angles are smaller when carbon is used in the system.

During the first stage, the rate of spreading decreases from an initially large value. Consequently, during the first stage, liquid Al remains in contact in the vicinity of the triple point, with a virtually unreacted surface where $\theta_1 > 100°$ for the three samples (Table 2). In the third stage, the ratio of the work of adhesion for Al on Al_2O_3 to the work of cohesion of Al ($2\gamma_{l-v}$) is 0.56, 0.65 and 0.88 for samples A1, AC1 and AC3, respectively. Such high values, principally those of samples with carbon, cannot be interpreted on the basis of weak interactions. These results are comparable with those obtained by others in similar measurements in systems with carbon.[29,34,35] In this work no detailed analyses have been carried out to verify the presence of Al_4C_3 at the interface. However, it is possible to say that the presence of carbon has promoted wetting but the mechanisms remains to be determined.

Table 2. Contact angles with the corresponding works of adhesion at each stage

Sample	θ_1	θ_2	θ_3	W_{ad2}	W_{ad3}
A1	119°	—	83°	—	0.954
AC1	110°	79°	72°	1.01	1.11
AC3	112°	55°	40°	1.34	1.50

Spreading

In experiments with sample A1 the contact angle varies from 119° to a minimum value of 82°. After 600 s the sample reached a quasi-steady regime with a contact angle of 83°, which remained almost constant for subsequent times. Scanning electronic microscopy analysis of the substrate after removing the Al drop (Fig. 4) revealed a series of rings on the Al_2O_3 surface interface between the metal and the ceramic. Each ring corresponds to a jump of the leading edge of the molten Al droplet during the spreading process. A detailed analysis of the micrograph in Fig. 4 shows that the separation of these rings increases with the distance away from the center of the Al drop. These rings are formed relatively fast (~600 s) during the first stage in Figs 3(a) and 3(b).

After removing the Al drop from sample AC3 (processed at 1300 °C for 4500 s), observations of the interfacial region between the metal and ceramic substrate were carrying out using SEM in the backscattered mode. Figure 5 shows significant microstructural differences. An interface between Al and Al_2O_3 is clearly defined and corrosion of Al_2O_3 by the liquid Al during the sessile drop experiment is evident by the good definition of the Al_2O_3 grain boundaries (Fig. 5(a)).

Energy-dispersive spectroscopy analysis performed in the three zones did not reveal any detectable difference in the concentration of Al, C and O, therefore the presence of components such as Al_4C_3 formed as a product of reaction between carbon and Al cannot be determined conclusively, as suggested by the reaction

$$4Al + 3C \rightarrow Al_4C_3 \quad (\Delta G = -203\ \mathrm{kJ\ mol^{-1}}) \qquad (4)$$

However, the metal/substrate interface is rougher than the substrate and holes of different sizes are present in the microstructure, principally in the interface. The presence of the roughened surface and these voids are an indication that reactions have occurred. The advance of the reaction front is marked by the extension of the interface. Figure 5(b) shows a ring at the edge of the interface where the substrate begins. This ring marks the edge of the liquid Al spreading front on Al_2O_3. Some authors report that the formation of Al_4C_3 is responsible for the wetting enhancement in this kind of system[28–32] but Al_4C_3 could have been dissolved during removal of the Al drop from the substrate by the reaction

$$Al_4C_3 + 12H_2O \rightarrow 4Al(OH)_3 + 3CH_4 \uparrow \qquad (5)$$

We do not believe that this compound was formed during these experiments because, under the experimental conditions, it is very unstable and the greatest reduction in contact angle was realized without direct evidence of the formation of a carbide phase. Therefore, an alternative explanation is that the improved wetting in the system could be due to the dissolution of carbon in Al owing to the solubility of carbon in liquid Al, which is >0.71 at.% at temperatures above 1200 °C.[36] This means that a gradient in concentration of carbon in Al is created, which facilitates the diffusion of liquid Al into the reaction layer. On the interface, a complex arrangement of phases is present in the cooled sample. This complex arrangement of phases, coupled with penetration of the Al_2O_3 grain boundaries by the liquid Al, suggests that reactions between the liquid Al and the carbon-coated Al_2O_3 substrate occurred during the sessile drop experiment. Reactions lead to a change in composition of the liquid that can change the interfacial energies significantly for spreading to take place.

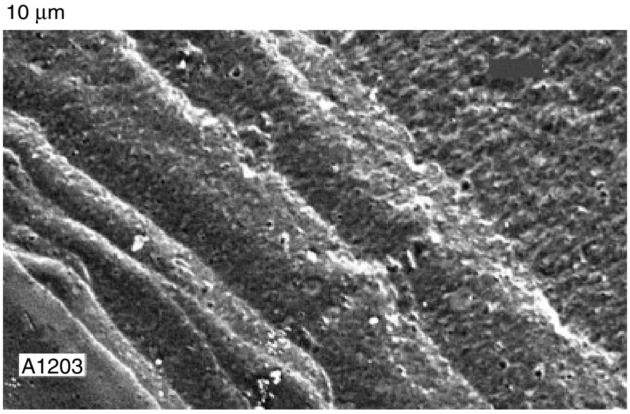

Figure 4. Scanning electron micrograph showing a succession of reaction rings in sample Al, delineated by triple line ridges (processed at 1300 °C for 4500 s).

Control mechanism

The rate of wetting can be controlled by an interfacial process or by diffusion. In diffusion-controlled wetting of a solid

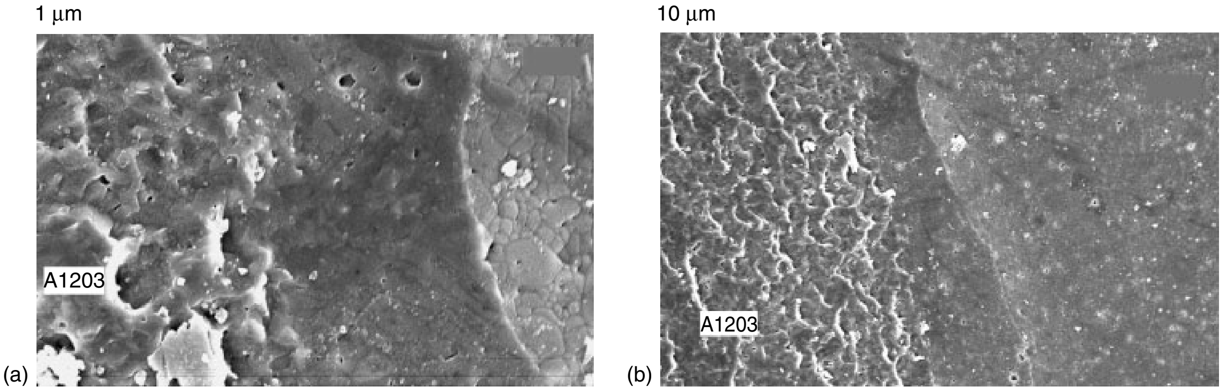

Figure 5. Scanning electron micrographs showing the metal/ceramic interface in sample AC3. Experimental conditions: 1300 °C for 4500 s.

the metal/ceramic interface increases linearly with time (constant wetting rate; see Fig. 3). When diffusion is rapid, the concentration is nearly constant and the interfacial process controls the rate of wetting, whereas for a rapid interfacial reaction the concentration profile is that for diffusion. Equation (6) is derived for different boundary conditions by Doremus[37] and gives the conditions to establish mechanism control in the process of wettability

$$C_R = \frac{C_I - C_E}{1 + \alpha X/D} + C_E \tag{6}$$

where C_R is the interface concentration, C_I is the initial concentration, C_E is the equilibrium concentration, X is the thickness of the interface, D is the diffusion coefficient and α is a coefficient with units cm s^{-1}.

When $\alpha X/D \ll 1$ there is interface control (diffusion is rapid compared with reaction) and $C_R \rightarrow C_I$; when $\alpha X/D \gg 1$ there is diffusion control and $C_R = C_E$. These results show that the thickness of the interface can influence strongly the mechanism of wetting. Thick interfaces favor diffusion control because of longer diffusion distances, and small thickness interfaces favor interface control.

In order to verify the control mechanism in this experiment the factor $\alpha X/D$ of Eqn (6) was estimated for samples A1, AC1 and AC3 under different conditions (data of α and D were obtained from the literature).[21] The results of these calculations suggest that diffusion is the mechanism controlling the wetting behavior in this system. This is well established because the temperature dependence of the reaction rate constant follows an Arrhenius equation $k = k_o \exp(-Q/RT)$, as expected from its major dependence on diffusion coefficient and temperature (see Fig. 2). A parabolic rate law is commonly observed for the kinetics process in which the limiting step is mass transport (Al diffusion) through a reaction layer (thickness of the interface; see Figs 4, 5 and 6). The thickness of the interface is a function of the square root of time

$$X = kt^{1/2} \tag{6}$$

SUMMARY

The sessile drop technique was used to study the influence of carbon on the interface contact angle between alumina and liquid Al. Experiments revealed initial contact angles close to 119°, which is characteristic of the non-reactive Al–Al_2O_3 system. After ~600 s this angle diminishes to a value of 83° for the uncoated-Al_2O_3 sample and after 2700 s to 79° and 55° for Al_2O_3 samples coated using one and three carbon deposition cycles, respectively, producing an energetically weak interface. In the absence of a carbon film there were no significant changes in the magnitude of the contact angle, even at times as long as 7200 s. On the other hand, coated samples after 4500 s reached minimum contact angle values of 72° and 40° for one and three carbon deposition cycles in Al_2O_3, respectively. The interpretation of this wetting behavior is that the contact angle reduction is driven by reactions between the liquid Al and the carbon-coated-Al_2O_3 substrate, taking into consideration that the work of adhesion for the final contact angle represents a high fraction of the work of cohesion of Al, owing to a strong interaction between liquid Al and carbon. However, the true mechanism by which carbon enhances the wetting of Al_2O_3 by liquid Al remains unclear and further research is necessary to try to establish what kind of reactions are occurring at the liquid Al/Al_2O_3 interface when carbon-coated Al_2O_3 substrates are used.

Acknowledgements

The authors are grateful for the assistance provided by Dr Michael Santella and Alan Frederick of Oak Ridge National Laboratory during the experimental phase of this work. One of the authors (E.R.R.) acknowledges the support of UAM-A, Conacyt and DOE for his postdoctoral research at ORNL.

REFERENCES

1. Cornie JA, Chiang YM, Uhlmann DR, Mortensen A, Collins JM. *Am. Ceram. Soc. Bull.* 1986; **65**: 293.
2. Wang DJ, Wu ST. *Acta Metall. Mater.* 1994; **42**: 4029.
3. Laurent V, Chatain D, Chatillon C, Eustathopoulos N. *Acta Metall.* 1988; **36**: 1797.
4. Ownby PD, Li KWK. *J. Am. Ceram. Soc.* 1991; **74**: 1275.
5. Eustathopoulos N, Chatain D, Coudurier L. *Mater. Sci. Eng.* 1991; **A135**: 83.
6. John H, Hausner H. *Int. J. High Technol. Ceram.* 1986; **2**: 73.
7. John H, Hausner H. *J. Mater. Sci. Lett.* 1969; **5**: 569.
8. Weirauch DA. *Ceramic Microstructures'86*, Pask JA, Evans AG (eds). Plenum Publishing Co.: New York, NY, 1988; 329.
9. Weirauch DA Jr. *J. Mater. Res.* 1998; **3**: 729.
10. Kubaschewski O, Hopkins BE. *Oxidation of Metals and Alloys* Butterworths, London, 1962.
11. Fujii H, Nakae H, Okada K. *Acta Metall. Mater.* 1993; **41**: 2963.
12. Saiz E, Cannon RM, Tomsia AP. *Acta Mater.* 2000; **48**: 4449.
13. Li J. *J. Am. Ceram. Soc.* 1992; **75**: 8.
14. Nicholas MG, Valentine TM, Waite MJ. *J. Mater. Sci.* 1980; **15**: 2167.
15. Loehman RE, Tompsia AP. *Acta Metall. Mater.* 1992; **40**: S75.
16. Weirauch DA Jr, Krafick WJ. *Metall. Trans. A* 1990; **21A**: 1745.
17. Young T. *Philos. Trans. R. Soc.* 1805; **95**: 65.
18. Kritsalis P, Coudurier L, Eustathopoulos N. *J. Mater. Sci.* 1991; **26**: 3400.
19. Loehman R. *Am. Ceram. Bull.* 1989; **68**: 891.
20. Kang S. *Am. Ceram. Bull.* 1989; **68**: 1608.
21. Aksay IA, Hoge CE, Pask JA. *J. Phys. Chem.* 1974; **78**: 1178.
22. Delannay F, Froyen L, Deruytterre A. *J. Mater. Sci.* 1987; **22**: 1.
23. Chidambaram PR, Edwards GR, Olson DL. *Metal. Trans. B* 1992; **23B**: 215.
24. Brennan JJ, Pask JA. *J. Am. Ceram. Soc.* 1968; **51**: 569.
25. Champion JA, Keene BJ, Sillwood JM. *J. Mater. Sci.* 1969; **4**: 39.
26. Scott PM, Nicholas M, Dewar B. *J. Mater. Sci.* 1975; **10**: 1833.
27. Eustathopoulos N. *Acta Mater.* 1998; **46**: 2319.
28. Landry K, Eustathopoulos N. *Acta Mater.* 1996; **44**: 3923.
29. Landry K, Kalogeropoulou S, Eustathopoulos N, Naidich Y, Krasovsky V. *Scr. Mater.* 1996; **34**: 841.
30. Keene BJ. *J. Int. Mater. Rev.* 1993; **38**: 157.
31. Garcia-Cordobilla C, Louis E, Pamies AJ. *J. Mater. Sci.* 1986; **21**: 2787.
32. Goumiri L, Joud JC. *Acta Metall* 1982; **30**: 1397.
33. McComb DW, Ning X-G, Weatherly GC, Pan J, Lloyd DJ. *Philos. Mag. A* 2000; **80**: 2509.
34. Drevet B, Kalogeropoulou S, Eustathopoulos N. *Acta Metall. Mater.* 1993; **41**: 3119.
35. Pech-Canul MI, Katz RN, Makhlouf MM, Pckard S. *J. Mater. Sci.* 2000; **35**: 2167.
36. Massalsk TB. *Binary Alloy Phase Diagrams* (2nd edn). ASM International: Materials Park, OH, 1990; 130.
37. Doremus RH. *Rates of Phase Transformations*. Academic Press: Inc., Orlando, FL, 1985; 4.